PCCP

Electron transfer in extended systems: characterization by periodic density functional theory including the electronic coupling

Journal:	*Physical Chemistry Chemical Physics*
Manuscript ID	CP-ART-09-2019-005133.R1
Article Type:	Paper
Date Submitted by the Author:	12-Oct-2019
Complete List of Authors:	Behara, Pavan Kumar; University at Buffalo - The State University of New York, Department of Chemical and biological engineering, Computational and Data-enabled Science and Engineering Program Dupuis, Michel; University at Buffalo - The State University of New York, Department of Chemical and biological engineering, Computational and Data-enabled Science and Engineering Program

Electron transfer in extended systems: characterization by periodic density functional theory including the electronic coupling

Pavan Kumar Behara and Michel Dupuis
Department of Chemical and Biological Engineering
Computational and Data-Enabled Science and Engineering Program
University at Buffalo, State of New York University
Buffalo NY 14260

Abstract:

We describe a new computer implementation of electron transfer (ET) theory in extended systems treated by periodic density functional theory (***DFT***), including the calculation of the electronic coupling transition element V_{AB}. In particular, the development opens up the full characterization of electron transfer in the solid state. The approach is valid for any single-determinant wavefunction with localized character representing the electronic structure of the system, from Hartree-Fock (***HF***) theory, to density functional theory (***DFT***), ***hybrid DFT*** theory, ***DFT+U*** theory, and constrained ***DFT*** (***cDFT***) theory. The implementation in CP2K reuses the high-performance functions of the code. The computational cost is equivalent to only one iteration of an ***HF*** calculation. We present test calculations for electron transfer in a number of systems, including a 1D-model of ferric oxide, hematite Fe_2O_3, rutile TiO_2, and finally bismuth vanadate $BiVO_4$.

1. Introduction:

The theory of electron transfer (ET) in gas and solution phases has a very long history, dating back to the work of Hush and collaborators[1] and Marcus and collaborators.[2-8] Fundamentals of the Marcus model have been investigated in numerous computer simulations of redox reactions in solution[9-18] with a focus on the characterization of the free energy surface, and dealing much less with the electronic coupling. A number of reviews are also available about electron transfer investigated by computation and simulation in biochemistry.[19-22] Modeling of charge transport in the solid state (polarons) has also a long history, with the seminal work of Friedman and Holstein[23], Emin and Holstein[24,25], Austin and Mott[26], and Emin[27-30] for example, and DFT calculations reported in recent years.[31-34] At the intersection of the solid state and chemistry, the structure and transport of charge carriers in conducting polymers have been at the forefront of research for many years.[35-43] Indeed the experimental work spurred a great deal of theoretical efforts toward the characterization of carriers by Su, Schrieffer, and Heeger[44,45] with extensions by Bredas and collaborators in many areas of organics, including organic photovoltaics.[46-53] Beyond these studies recent years have seen a growing interest in obtaining molecular-level details of redox chemistry at oxide surfaces in electrolyte environments.[31,54-63] Lastly, the recent push for renewable energy and efficient solar-to-electricity and solar-to-fuel conversion materials, has greatly increased the interest in understanding and manipulating carrier transport in inorganic semi-conductors. [32,64-72] Several of these studies showed already that polaron diffusion mobility extracted from Einstein diffusion model and DFT-derived ET rates can be within one order of magnitude of experimental values[31,32,64] with energy barriers within ~ 0.05 eV from experimental values. We refer the reader to the papers and reviews referenced above to experience the breadth of applications involving ET computation and simulation.

The work described in the present paper deals with a technical development that enables ET computation in all of these domains, although the driving force for our research has been the computation of electron transfer in the solid state. A growing number of studies have appeared about carrier transport in the literature, most focusing on energetics parameters such as stability and reorganization energy (in Marcus/Holstein parlance). They often leave out the electronic coupling $\boldsymbol{V_{AB}}$ that in fact plays a key role as a descriptor of the diabatic or adiabatic nature of ET as well as enters the rate expression. In a limited number of these studies, the authors resorted to cluster models to evaluate the electronic coupling. The present work overcomes this shortcoming.

Theoretical studies of ET with ***n***-electron wavefunctions started with Newton and collaborators using localized quasi-diabatic (non-orthogonal) states [13-15,73,74]. Various approaches to calculating the electronic coupling element were developed[75-78] and several molecular implementations have been available for some time.[79,80] Many studies using semi-empirical or *ab initio* Hartree-Fock (HF) theories have been reported.[81-83] With the advent of density functional theory[84,85] (DFT) and the development of the constrained DFT method (***cDFT***), the interest has shifted to ET described with DFT and cDFT,[86-91] both for molecules and organic solids. [34,92-99] Different approaches are used to 'localize' the initial and final states of ET, including charge- or spin-constrained DFT or fragment-based localization. For a recent review, see the work of Oberhofer *et al.*[34]

In the present research, our starting point for localized quasi-diabatic non-orthogonal ***n***-electron states are molecular or periodic ***DFT*** Kohn-Sham wavefunctions with correction for self-interaction error (hybrid functional ***DFT*** [100,101] or ***DFT+U*** [102,103]). Like with ***HF*** theory, they offer a means to obtain localized states without external constraints. Note that our formalism is not

limited by this 'requirement' and can treat ***cDFT*** or fragment-projected states as well. We aim to calculate the electronic coupling matrix element for any type of quasi-diabatic ***DFT***-based states in molecular or periodic DFT calculations. The present implementation involves a slightly simplified form of the Farazdel formulation[80] for spin-unrestricted ***HF*** wavefunctions, using the corresponding orbitals transformation.[104] The present work goes beyond the recent work of Bylaska and Rosso[105] in that we can treat periodic ***DFT***-based wavefunctions, including ***hybrid*** functional wavefunctions for molecules and periodic solids, ***DFT+U*** wavefunctions, and ***cDFT*** wavefunctions, that are popular in the solid state community. We note that, beyond the issue of the often prohibitive cost of periodic ***HF*** calculations, the use of ***HF*** theory is problematic as it does not account for strong correlation effects existing, for example, in semiconductors.

The paper is organized as follows: in section II we present the equations for the electronic coupling element valid in a molecular case and in a periodic case. In section III we give details of the implementation in the CP2K code that uses Gaussian-type basis functions as the expansion set of the one-electron Kohn-Sham (KS) states. In section IV we present and discuss results for a number of benchmark systems, including hole transfer in He_2^+ and Zn_2^+, electron polaron transfer

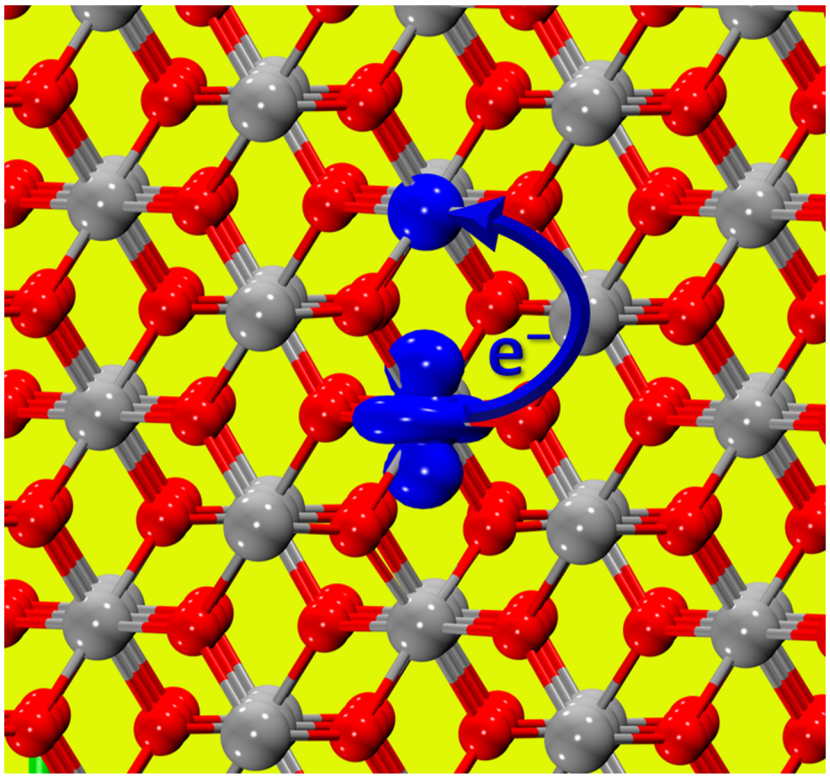

Figure 1. Spin density of an electron polaron localized on a Ti site in TiO_2. We aim to calculate the rate for the polaron to hop between two Ti sites. The blue spheres are polaronic Ti atoms, the red spheres are O atoms, and the silver spheres are Ti atoms.

in a 1D chain of OH-bridged Fe^{III} ions, in bulk rutile TiO_2, and in bulk hematite Fe_2O_3, and lastly in bismuth vanadate $BiVO_4$. In ***Appendix A*** we elaborate on our choice of the exact ***n***-electron Hamiltonian for the calculation of V_{AB} as it removes a theoretical ambiguity. In ***Appendix B*** we give essential details of the code implementation.

2. Formulation and Implementation

For an excellent review of electron transfer theory, we refer the reader to the recent paper by Bylaska and Rosso. [105] An electron polaron transfer in an inorganic solid is depicted in Figure 1 (here TiO_2). We are interested in the rate of transfer (hopping) of the electron (polaron) from one Ti site to another. The localization of the excess electron density induces a lattice relaxation around the localization site. When the lattice relaxation is limited to the region near the localization site, we have what is known a small polaron.[25] Small polaron transport is prevalent in inorganic and organic semi-conductors.[47,106] In the two regimes of diabatic and adiabatic transfer, the hop involves a 'transfer' of the lattice distortion from one site to the other.

Just like for molecules, the system can be looked at as a double-well potential, the electron hops back and forth from one well to the next at some characteristic frequency which depends on the height of the potential barrier. A schematic representation of the potential energy surface (PES) of the system as a function of the nuclear coordinates $\boldsymbol{Q}$ is shown in Figure 2. The initial state $\boldsymbol{A}$ with the left-localized electronic state $\boldsymbol{\Psi_A}$ resides in a local minimum on the PES that corresponds to its equilibrium nuclear configuration $\boldsymbol{Q_A}$. The final state $\boldsymbol{B}$ with its right-localized electronic

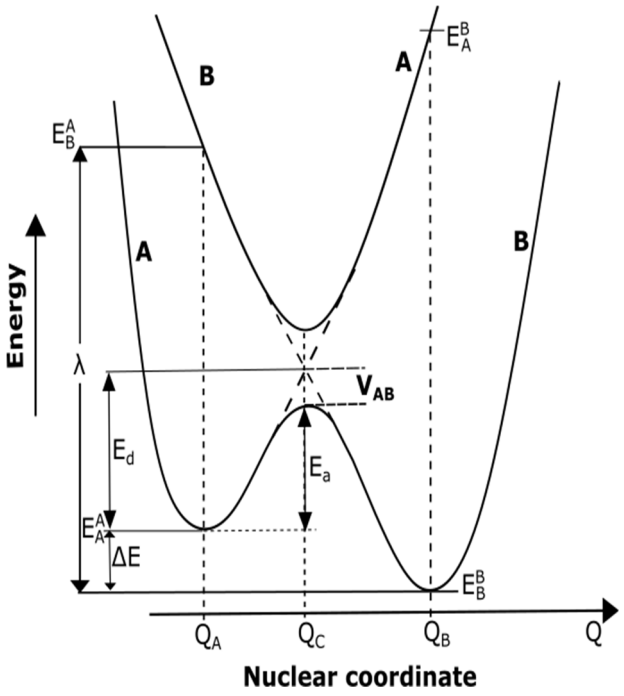

Figure 2. Schematic of the two-well potential energy surface associated with electron or hole transfer in molecules and in the solid state (reproduced from Farazdel et al. [71]). The solid curves are the adiabatic surfaces; the dashed lines depict the diabatic states. Q_A and Q_B are the equilibrium coordinates of the A state and B state, and Q_c represent the coordinates of the lowest energy structure on the crossing seam of the diabatic surfaces. λ is the reorganization energy, $|\Delta E|$ is the exothermicity of the electron transfer, E_d is the diabatic activation energy, E_a is the adiabatic activation energy, and V_{AB} is the electronic coupling between states A and B.

state $\boldsymbol{\Psi_B}$ resides similarly in a local minimum on the PES denoted $\boldsymbol{Q_B}$. The two minima may differ in energy, and the exothermicity is denoted ΔE.

The quantity $\boldsymbol{V_{AB}}$ shown in Figure 2 plays a key role in ET or polaron transfer theory. It is related to the "electronic coupling" $\boldsymbol{H_{AB}} = \langle \boldsymbol{\Psi_A} | \boldsymbol{H} | \boldsymbol{\Psi_B} \rangle$ between states $\boldsymbol{A}$ and $\boldsymbol{B}$, where $\boldsymbol{H}$ is the total $\boldsymbol{n}$-electron Hamiltonian (excluding the nuclear kinetic energy and nuclear repulsion terms). When $\boldsymbol{H_{AB}} = 0$, the two (diabatic) surfaces $\boldsymbol{A}$ and $\boldsymbol{B}$ intersect at a crossing seam where the states have the same energy and the same nuclear configuration. The ET is then a diabatic transition governed by the Franck-Condon principle with conservation of energy. When $\boldsymbol{H_{AB}} \neq 0$, the states $\boldsymbol{\Psi_A}$ and $\boldsymbol{\Psi_B}$ do not diagonalize the electronic Hamiltonian $\boldsymbol{H}$ and the degeneracy of the states is removed. We have an avoided crossing, the two surfaces are now adiabatic surfaces for $\boldsymbol{n}$-electron states $\boldsymbol{\Psi_+}$ and $\boldsymbol{\Psi_-}$ with energies $\boldsymbol{E_+}$ (upper state) and $\boldsymbol{E_-}$ (lower state) extracted from the 2×2 secular equation arising from writing the wavefunction of the system as a linear combination of the two quasi-diabatic states $\boldsymbol{\Psi_A}$ and $\boldsymbol{\Psi_B}$ in the framework of the two-state model:

$$\Psi_+(Q) = c_+^A(Q)\Psi_A(Q) + c_+^B(Q)\Psi_B(Q)$$
$$\Psi_-(Q) = c_-^A(Q)\Psi_A(Q) + c_-^B(Q)\Psi_B(Q)$$
$$H(Q)C_\pm(Q) = E_\pm(Q)S(Q)C_\pm(Q)$$
$$C_\pm(Q) = \begin{pmatrix} c_\pm^A(Q) \\ c_\pm^B(Q) \end{pmatrix}$$
$$H(Q) = \begin{pmatrix} H_{AA}(Q) & H_{AB}(Q) \\ H_{AB}(Q) & H_{BB}(Q) \end{pmatrix}$$
$$S(Q) = \begin{pmatrix} S_{AA}(Q) & S_{AB}(Q) \\ S_{AB}(Q) & S_{BB}(Q) \end{pmatrix} \quad (1)$$

with

$$H_{AA}(Q) = \langle \Psi_A(Q) | H(Q) | \Psi_A(Q) \rangle$$
$$H_{BB}(Q) = \langle \Psi_B(Q) | H(Q) | \Psi_B(Q) \rangle$$
$$H_{AB}(Q) = \langle \Psi_A(Q) | H(Q) | \Psi_B(Q) \rangle$$
$$S_{AA}(Q) = \langle \Psi_A(Q) | \Psi_A(Q) \rangle = 1$$
$$S_{BB}(Q) = \langle \Psi_B(Q) | \Psi_B(Q) \rangle = 1$$
$$S_{AB}(Q) = \langle \Psi_A(Q) | \Psi_B(Q) \rangle \quad (1a)$$

The secular equation has the form:

$$\begin{vmatrix} H_{AA} - E & H_{AB} - ES_{AB} \\ H_{AB} - ES_{AB} & H_{BB} - E \end{vmatrix} = 0 \quad (2)$$

The separation between the adiabatic surfaces is given by:

$$\Delta(Q) = E_+ - E_- = \frac{2}{(1-S_{AB}^2)}\left\{\begin{matrix}\frac{1}{4}(H_{AA}-H_{BB})^2 - (H_{AA}+H_{BB})H_{AB}S_{AB} \\ +H_{AA}H_{BB}S_{AB}^2 + H_{AB}^2\end{matrix}\right\}^{\frac{1}{2}} \quad (3)$$

and by convention

$$V_{AB} = \frac{1}{2}\Delta(Q = Q_C) = \frac{1}{(1-S_{AB}^2)}\left\{H_{AB} - \frac{S_{AB}(H_{AA}+H_{BB})}{2}\right\} \quad (4)$$

$\boldsymbol{V_{AB}}$ is a key quantity that appears in classical[3], semi-classical[107], and quantum mechanical[108,109] treatment of ET theory. The rate expression that ensues in the diabatic regime is [110]:

$$k_{ET} = \frac{2\pi}{\hbar}V_{AB}^2\frac{1}{(4\pi\lambda k_B T)^{\frac{1}{2}}}\exp\left(\frac{-[\lambda + \Delta E]^2}{4\lambda k_B T}\right) \quad (5)$$

and in the adiabatic case[31] it is:

$$k_{ET} = i\nu_n exp\left(\frac{-E_a}{k_B T}\right)$$

$$E_a = -\frac{\lambda}{4} + \frac{(\lambda^2 + 4V_{AB}^2)^{\frac{1}{2}}}{2} - V_{AB} \quad (6)$$

In both cases the rate can be determined from the knowledge of λ and $\boldsymbol{V_{AB}}$.

Differences among formalisms and implementations of ET lie in the nature of the quasi-diabatic $\boldsymbol{n}$-electron states $\boldsymbol{\Psi_A}$ and $\boldsymbol{\Psi_B}$ and in the expression used for the evaluation of the Hamiltonian elements $\boldsymbol{H_{AA}}$, $\boldsymbol{H_{BB}}$, and $\boldsymbol{H_{AB}}$. In the present work we use Kohn-Sham states to determine the quasi-diabatic states and we use the exact $\boldsymbol{n}$-electron Hamiltonian to determine the state mixing and their interactions. Important theoretical considerations governing these choices are expounded upon in the ***Appendix A*** below.

In brief, we needed to address two issues. The first one was related to the well-known self-interaction error of ***DFT*** that makes it hard to 'localize' electrons. We can use ***HF*** and ***hybrid DFT*** theory that are computationally expensive and at times prohibitive in periodic calculations. Alternately, we can use ***DFT+U*** theory that is computationally efficacious and yields charge or spin-localized states. For Hamiltonian operator, we use the exact $\boldsymbol{n}$-electron Hamiltonian (as we would for periodic ***HF*** theory) but we used the $\boldsymbol{n}$-electron KS determinants to set the secular equation of eq.(2). In essence, we calculate the ***HF*** energy and coupling term of the KS-***DFT*** states. Using the exact $\boldsymbol{n}$-electron Hamiltonian is now computationally affordable owing to the availability of efficient computer codes for periodic calculations that can treat the exact exchange of ***HF*** theory[111-113] and the fact that our $\boldsymbol{V_{AB}}$ calculation involves the equivalent of a single ***HF*** iteration, a very tractable cost. For molecular calculations the formalism is rather straightforward in contrast to periodic calculations that make use of Bloch states with their $\boldsymbol{k}$-points in the first Brillouin zone to account for periodicity.[114] the corresponding orbital transformation may be

carried out for each $\boldsymbol{k}$ point independently.[105] The present implementation in the CP2K code[115] deals solely with the $\boldsymbol{\Gamma}$ point.

Modified formulation of the corresponding orbital transformation for the calculation of the electronic coupling in ET in the solid state:

The difficulty in evaluating the interaction and overlap terms $\boldsymbol{H_{AB}}$ and $\boldsymbol{S_{AB}}$ between states $\boldsymbol{A}$ and $\boldsymbol{B}$ arises from the non-orthogonality of the ($\boldsymbol{1}$-electron states) orbitals $\boldsymbol{a}$ and $\boldsymbol{b}$. The corresponding orbital transformation (COT) of King *et al.*[104] defines a unitary transformation of the $\boldsymbol{a}$ orbitals of state $\boldsymbol{A}$ and another one for the $\boldsymbol{b}$ orbitals of state $\boldsymbol{B}$ that make the transformed orbitals mutually orthogonal between states $\boldsymbol{A}$ and $\boldsymbol{B}$, thus facilitating the calculation of $\boldsymbol{S_{AB}}$ and $\boldsymbol{H_{AB}}$:

$$
\begin{aligned}
a &= |\mu\rangle A \\
b &= |\mu\rangle B \\
D &= A^{\dagger}\langle\mu|\mu\rangle B \\
\hat{a} &= aV = \big|\mu\rangle\hat{A} \\
\hat{b} &= bU = \big|\mu\rangle\hat{B} \\
D &= \langle a|b\rangle \\
\hat{d} &= \big\langle\hat{a}\big|\hat{b}\big\rangle = U^{\dagger}DV
\end{aligned}
\tag{6}
$$

In eq.(6), $|\mu\rangle$ denotes the one-electron basis set used in the expansion of the $\boldsymbol{1}$-electron states $\boldsymbol{a}$ and $\boldsymbol{b}$. We obtain a generalized density matrix $\boldsymbol{P}$ from the transformed orbitals that enables the calculation of $\boldsymbol{1}$- and $\boldsymbol{2}$-electron contributions to the Hamiltonian matrix element $\boldsymbol{H_{AB}}$:

$$
\begin{aligned}
P &= \hat{A}T\hat{B} \\
\Omega_{AB}^{(1)} &= (detU)(detV^{\dagger})\sum_{\mu\nu}^{M} P_{\mu\nu}\omega_{\mu\nu}^{(1)} \\
\omega_{\mu\nu}^{(1)} &= \big\langle\chi_{\mu}\big|\omega^{(1)}\big|\chi_{\nu}\big\rangle \\
T_{ii} &= \prod_{j\neq i}^{N}\hat{d}_{jj} \\
prod &= \prod_{k=1}^{N}\hat{d}_{kk} \\
\Omega_{AB}^{(2)} &= \frac{1}{2}(detU)(detV^{\dagger})(prod)^{-1}\sum_{\mu\nu\lambda\sigma}^{M} P_{\mu\nu}P_{\lambda\sigma}\{\langle\mu\nu|\lambda\sigma\rangle - \langle\mu\sigma|\lambda\nu\rangle\}
\end{aligned}
\tag{7}
$$

We note that the generalized density matrix $\boldsymbol{P}$ is not symmetric due to the differently localized states $\boldsymbol{A}$ and $\boldsymbol{B}$. To take advantage of existing functionalities in CP2K that are extensively tuned for massively parallel processing, we have found it convenient to decompose $\boldsymbol{P}$ into a symmetric matrix and an anti-symmetric matrix:

$$P = P_{sym} + P_{anti}$$
$$P_{sym} = \frac{P + P^{\dagger}}{2}$$
$$P_{anti} = \frac{P - P^{\dagger}}{2} \quad (8)$$

a. Implementation in CP2K

We adapted the implementation by Farazdel in HONDO [116] to the CP2K [117] program, which can deal with periodic calculations. A summary of the steps includes:

1. Obtain the molecular orbitals of both states, $\boldsymbol{A}$ and $\boldsymbol{B}$, at a ***DFT/HF/Hybrid-DFT/cDFT/DFT+U*** level of theory in CP2K.
2. For both alpha and beta spins, do the following:
    a. Calculate the overlap matrix $\mathbf{D}$ from $\mathbf{D} = \mathbf{B}^{\dagger}\mathbf{S}\mathbf{A}$, where $\mathbf{A}$ and $\mathbf{B}$ are eigenvectors of the quasi-diabatic states obtained in step 1, and $\boldsymbol{S}$ is the overlap matrix over the atomic orbitals.
    b. Carry out the COT transformation (one for spin α, and one for spin β) by singular value decomposition of matrix $\mathbf{D}$, where $\mathbf{d} = \mathbf{U}^{\dagger}\mathbf{D}\mathbf{V}$.
    c. $\mathbf{U}$ and $\mathbf{V}$ are unitary matrices and their determinants are equal to one. This can be an internal check during implementation.
    d. Form the matrices $\widehat{\boldsymbol{A}}, \widehat{\boldsymbol{B}}, \boldsymbol{T}$, and the generalized density matrix $\boldsymbol{P}$.
3. Compute the overlap as $\boldsymbol{S_{AB}} = (\det \mathbf{U})(\det \mathbf{V}^{\dagger})$
4. Compute one-electron and two-electron energy contributions to $\boldsymbol{H_{AB}}$ by making use of CP2K functions for the efficient calculation of the Hartree potential and electron Coulomb energy as well as the ***HF*** exchange energy. In this step, we make use of the partitioning of the generalized density matrix into a symmetric and an anti-symmetric contribution. The relevant equations in CP2K are highlighted in Appendix B. Finally, compute $\boldsymbol{V_{AB}}$.

3. Application Examples

In this section we describe test calculations that can be compared with calculations performed with other codes or previously published calculations. The systems include He-He$^{(+)}$, Zn-Zn$^{(+)}$, a one-dimensional model of iron oxide, hematite Fe_2O_3, and TiO_2 rutile. Lastly we calculate $\boldsymbol{V_{AB}}$ for an electron polaron transfer in $BiVO_4$, a semiconductor with strong photocatalytic efficiency.[67,68] All the pictorial representations of atomic systems were made using VMD visualization software. [118]

3.a He_2^+ dimer

We calculated the electronic coupling for electron transfer in a helium dimer cation He-He$^{(+)}$ using the ***HF*** level of theory in CP2K and our new implementation of $\boldsymbol{V_{AB}}$. We selected a minimal basis set [119] for these all-electron calculations. Results at different inter-nuclear distances were validated

against the Hondo implementation[80] and are shown in Table 1. The data show excellent numerical agreement with the molecular code (differences less than 10^{-4} of the magnitude of V_{AB}, in particular ~ 0.1 cm^{-1} out of ~5000 cm^{-1}). What matters here is the excellent numerical accord. These results validate the correctness of the new V_{AB} module based on the Coulomb engine in CP2K.

He-He(+)	CP2K	CP2K	HONDO	HONDO
r (Å)	V_{AB} [cm^{-1}]	$\|S_{AB}\|$	V_{AB} [cm^{-1}]	$\|S_{AB}\|$
2.0	5373.714	5.1471E-01	5373.820	5.1472E-01
2.5	1754.505	1.5906E-01	1754.527	1.5907E-01
3.0	550.378	4.9504E-02	550.381	4.9505E-02
3.5	167.995	1.5075E-02	167.995	1.5075E-02
4.0	48.060	4.3110E-03	48.060	4.3105E-03
5.0	2.425	2.1647E-04	2.425	2.1789E-04
6.0	0.051	4.5515E-06	0.051	4.5927E-06

*Table 1. He_2^+ electronic coupling calculated in CP2K via the COT method with **HF** orbitals, compared with HONDO values for the same method.*

3.b Zn_2^+ dimer

We calculated the electronic coupling V_{AB} for electron transfer in a zinc dimer cation, Zn-$Zn^{(+)}$, again using the ***HF*** level of theory in CP2K. The hole occupies the ***4s*** atomic states of Zn in the left-localized and right-localized states. Both all-electron and pseudopotential calculations were performed and results are given in Table 2. We used the DZVP-ALL basis set provided with CP2K [119] for the all-electron calculations. We also used the zinc GTH pseudopotential [120-122] and associated basis set with 12 valence electrons. The two levels of theory, GAPW and GPW that use pseudo potentials yield results in very close numerical accord. The all-electrons results are somewhat larger. We attribute this fact to the basis set which is different between the all-electron and the pseudo-potential calculations. The values of V_{AB} decrease with increasing inter-nuclear distance. Our calculations are in good qualitative accord with the work of Wu and Van Voorhis using cDFT[88] and the work of Cave and Newton using the Generalized-Mulliken-Hush (GMH) approach.[76]

Zn-Zn(+)	GAPW All electron	GAPW with Pseudo-potential	GPW with Pseudo-potential	cDFT	GMH
	This work	This work	This work	Ref. 79	Ref. 67
R(Å)	V_{AB} [cm^{-1}]	V_{AB} [cm^{-1}]	V_{AB} [cm^{-1}]	V_{AB} [cm^{-1}]	V_{AB} [cm^{-1}]
5.0	1468.753	1227.365	1227.216	1245.491	1593.386
6.0	445.603	279.808	279.797	303.899	474.065
7.0	124.676	56.300	56.300	74.560	136.733
8.0	30.781	8.720	8.720	13.908	37.530
9.0	6.635	1.006	1.006	3.301	9.657

	$\|S_{AB}\|$	$\|S_{AB}\|$	$\|S_{AB}\|$		
5.0	6.1150E-01	6.7675E-01	6.7675E-01		
6.0	1.8670E-01	1.5434E-01	1.5433E-01		
7.0	5.2945E-02	3.2611E-02	3.2611E-02		
8.0	1.3147E-02	5.1359E-03	5.1358E-03		
9.0	2.8482E-03	5.9190E-04	5.9186E-04		

*Table 2. Electronic coupling **V_{AB}** and overlap **S_{AB}** calculated for Zn_2^+ with CP2K via the COT method using **HF** orbitals in this work, compared to **cDFT** orbitals in ref. 79 and the **GMH** formalism in ref. 67.*

3.c One-dimensional periodic iron oxide chains

We used CP2K to calculate V_{AB} in one-dimensional periodic chains of 7, 9, and 11 $Fe(OH)_2(H2O)_2^{(+)}$ units with one excess electron, following the work of Bylaska and Rosso. [105] The excess electron was localized on one of the Fe^{III} atoms making it Fe^{II}, thus the net effective charges on the 7-, 9-, and 11-unit cells were +6, +8, and +10 respectively. In these model systems, the iron atoms are in ferric high spin $3d^5$ states.

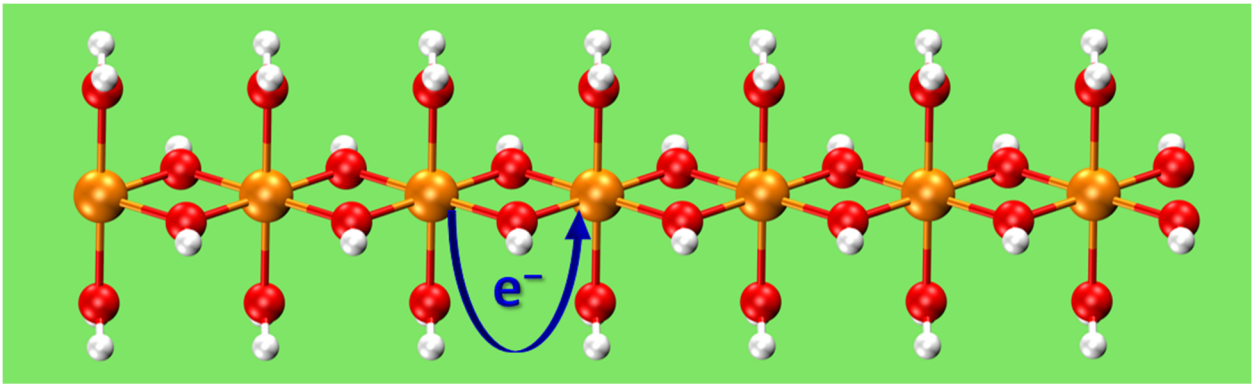

Figure 3. Structure of the ferric oxide 1D-model with 7 units. The system is periodic. The excess electron is localized on the third Fe atom in state A and transfers to the fourth Fe atom in state B (as depicted with the blue arrow). The orange spheres are Fe atoms, the red spheres are O atoms, and the white spheres are H atoms.

The localized character of the ***A*** and ***B*** states was monitored through the Mulliken spin population of the Fe *3d* atomic shells, high spin $3d^4$ for Fe(II) with the localized electron vs. high spin $3d^5$ for Fe(III). The lengths of the respective unit cells were 21.385 Å, 27.495 Å, and 33.605 Å in the X-direction. In the Y- and Z- directions, we used a box size of 35 Å.

The calculations were done using the ***GPW*** method and the ***HF*** level of theory for direct comparison with Bylaska-Rosso.[105] A truncated potential with cutoff radius equal to half of the smallest cell parameter was used for both ***HF*** and V_{AB} calculations. A modified DZV basis set [119] (in which we removed the ***f*** polarization functions from the Fe basis set, the ***d*** functions from the O basis set, and the ***p*** functions from the H basis set) and GTH pseudopotentials [120-122] were used for Fe, O and H atoms. The results are given in Table 3.

In these calculations (and the calculations below for hematite, rutile, and bismuth vanadate), we calculated the nine intermediate points along the selected reaction pathway, in addition to calculating states ***0*** (state ***A***) and ***1*** (state ***B***). ΔG* given in the table refers to the energy of the mid-point along the 'reaction pathway'. λ is the reorganization energy which is the energy gap between the left-localized state at its optimized geometry (state ***0***) and the right-localized state at the optimized geometry of state ***0***. In accord with Marcus theory, ΔG* and λ/4 ought to be equal when the states are quasi-diabatic, with a harmonic potential, and the ET process is thermo-neutral (localized on a single site). That this is the case in our calculation can be seen in Table 3. The adiabatic barrier is equal to (ΔG* - V_{AB}) .

1D $Fe^{(III)}$ model (***HF*** theory)	7 units (this work)	9 units (this work)	11 units (this work)	7 units (ref. 97)	9 units (ref. 97)	11 units (ref. 97)
ΔG* (eV)	0.531	0.544	0.528	0.562	0.544	0.607
λ/4 (eV)	0.521	0.539	0.518	0.521	0.528	0.524
V_{AB} (eV)	0.257	0.239	0.265	0.218	0.222	0.226
Adiabatic barrier (eV)	0.273	0.305	0.263	0.326	0.340	0.381
Overlap $\|S_{AB}\|$	0.088	0.081	0.091			

*Table 3. V_{AB} for ET of an electron polaron in a 1D periodic chain $[Fe(OH)_2(H2O)_2^{(+)}]_n$ with n=7, 9, and 11 units calculated with the **HF** level of theory. ΔG* is the relative energy of the mid-point along the reaction pathway, λ is the reorganization energy, V_{AB} is the electronic coupling, and the adiabatic barrier is equal to (ΔG* - V_{AB})*

In Figure 4 we display the alternating character of the Fe-(OH) bonds along the chain for the CP2K optimized electron polaron state localized on a Fe atom at the middle of the 11-unit chain obtained with the ***HF*** level of theory.

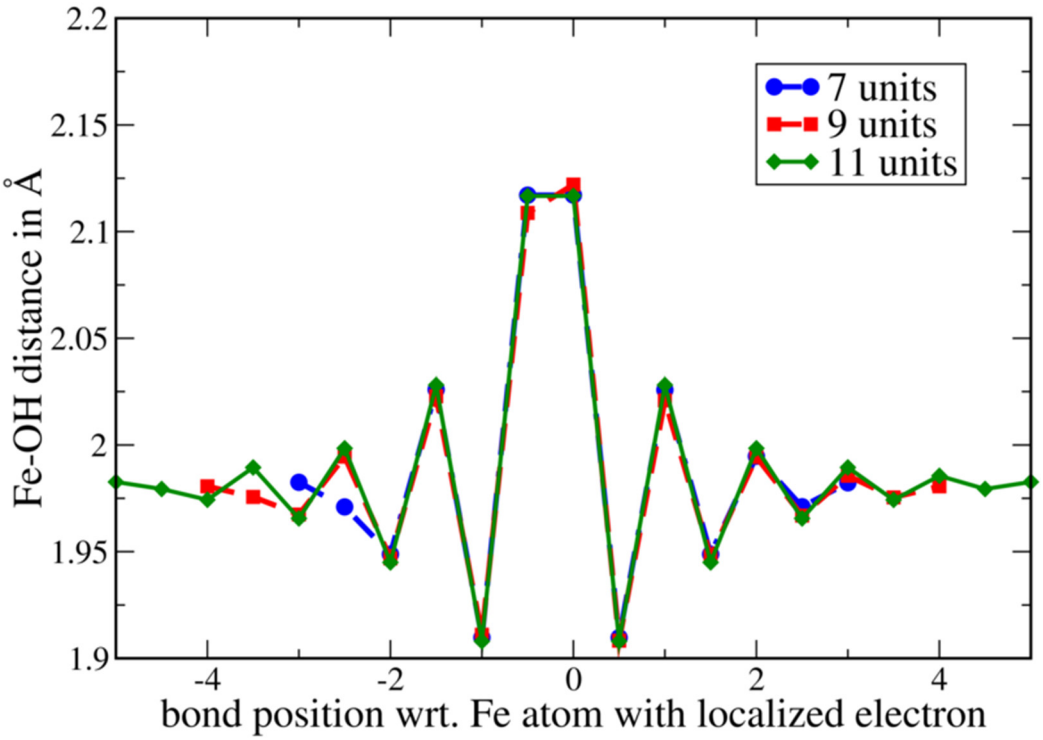

*Figure 4. Fe-OH bonds along the chain. The localized excess electron is at position **0**. The distances in the 7 and 9 unit systems are not distinguishable from those of the 11-unit system.*

The results are in good agreement with the work of Rosso and Dupuis[123] and Bylaska and Rosso[105], all of them using ***HF*** theory but different basis sets. The polaronic wave of bond length alternations attenuates at ~ five Fe atoms away from the reduced Fe atom.

For the 7-unit system, we used also the BLYP+U level of theory[124,125] with different +U values on the *3d* atomic orbitals of Fe. The results are shown in Table 4. Here the wavefunction accounts for some electron correlation effects, leading to a lowering of the diabatic barrier. With increasing +U values (on Fe), the overlap S_{AB} decreases, a sign that the excess electron resides in an orbital that is more and more tightly localized.

	BLYP+U U = 5	BLYP+U U = 6	BLYP+U U = 7	BLYP+U U = 8	BLYP+U U = 9	BLYP+U U = 10
ΔG* (eV)	0.443	0.444	0.443	0.441	0.469	0.469
λ/4 (eV)	0.405	0.407	0.383	0.391	0.424	0.425
V_{AB} (eV)	0.127	0.172	0.178	0.178	0.171	0.160
Adiabatic barrier (eV)	0.317	0.273	0.265	0.263	0.297	0.310
Overlap $\|S_{AB}\|$	0.329	0.179	0.115	0.084	0.063	0.048

Table 4. V_{AB} for a periodic chain of 7-units $[Fe(OH)_2(H2O)_2^{(+)}]_7$ calculated with BLYP+U orbitals and different +U value. ΔG is the energy of the mid-point along the reaction pathway, λ is the reorganization energy, V_{AB} is the electronic coupling, and the adiabatic barrier is equal to (ΔG* - V_{AB})*

3.d Bulk hematite Fe_2O_3

We calculated $\boldsymbol{V_{AB}}$ for electron transfer in the basal plane of bulk hematite, using the BLYP+U orbitals level of theory. A 3x3x1 supercell was used with cell parameters [a=14.725 Å, b=14.725 Å, c=13.267 Å], and [α=90, β=90, γ=120]. A modified DZV basis set [119] (DZVP basis set without ***f*** polarization functions on Fe and without ***d*** functions on O) was used for both Fe and O atoms along with GTH pseudopotentials.

An excess electron was localized on one of the Fe atoms as state ***A*** and on a neighbor Fe atom in the basal plane as state ***B***. We used $+U_{eff}$ values = 6.0 eV, 8.0 eV, and 10.0 eV applied to the ***3d*** orbitals of Fe. Iordanova *et al.* [126] reported a value of $\boldsymbol{V_{AB}}$ ~ 0.19 eV for a basal plane hop in high spin configuration, to be compared to ~ 0.04 eV obtained here. We note that the reorganization energy calculated with BLYP+U increases with the value of +U. It remains smaller than with the ***HF*** theory. The diabatic barrier ΔG* is found to be somewhat smaller with periodic BLYP+U theory than with cluster ***HF*** theory. $\boldsymbol{V_{AB}}$ is smaller with BLYP +U compared with cluster ***HF***. Overall the accord is satisfactory given the differences in levels of theory between the two calculations (cluster ***HF*** vs. periodic ***BLYP+U***), in basis sets, and lastly in the use of a cluster model for the $\boldsymbol{V_{AB}}$ calculation by Iordanova *et al.*

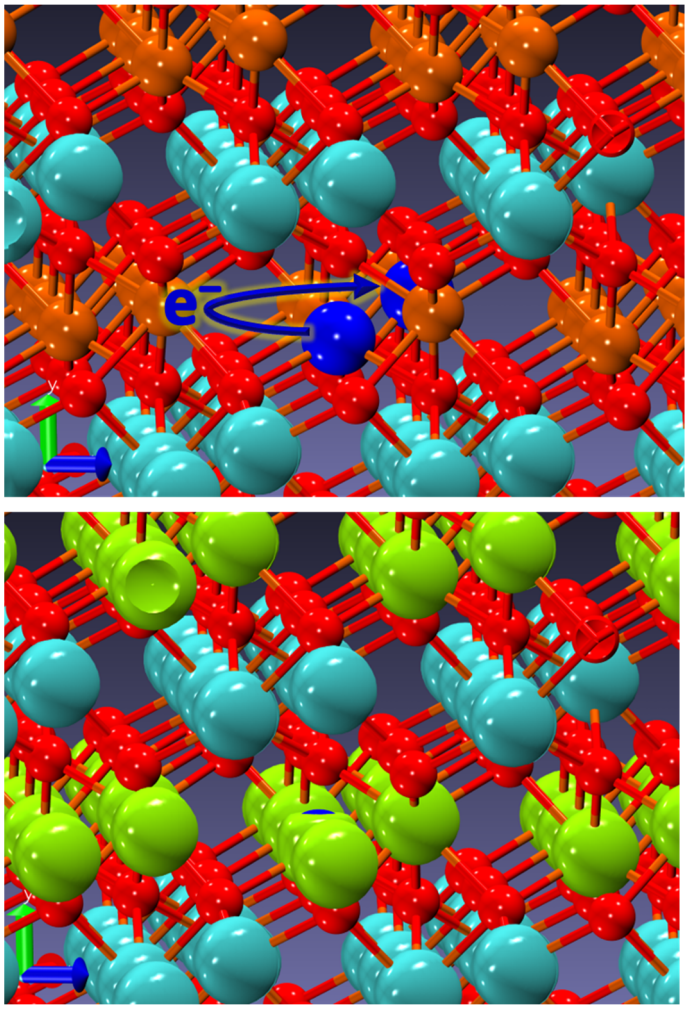

Figure 5. Fe_2O_3 hematite supercell with layers of spin-up [blue ■] and spin-down [green ■] densities on Fe^{III} atoms. The hop between two Fe atoms in a basal plane is marked in blue color. For clarity, the spin density contours are turned off for the down spin in the top picture. The orange spheres are Fe atoms, the red spheres are O atoms.

Hematite Fe_2O_3	BLYP+U, U = 6 eV	BLYP+U, U = 8 eV	BLYP+U, U = 10 eV	***HF*** cluster Ref. 117
ΔG* (eV)	0.218	0.265	0.290	0.380
λ/4 (eV)	0.200	0.253	0.294	0.355
V_{AB} (eV)	0.040	0.042	0.045	0.190
Adiabatic barrier (eV)	0.178	0.223	0.245	0.190
Overlap $\|S_{AB}\|$	0.023	0.016	0.011	

Table 5. V_{AB} for electron transfer in basal plane for bulk hematite from BLYP+U orbitals using CP2K. ΔG is the energy of the mid-point along the reaction pathway, λ is the reorganization energy, V_{AB} is the electronic coupling, and the adiabatic barrier is equal to (ΔG* - V_{AB}).*

3.e Bulk rutile TiO_2

This test calculation involved $\boldsymbol{V_{AB}}$ for electron transfer in the ***c***-direction for bulk rutile TiO_2. We used a ***DFT+U*** level of theory based on the PBE exchange correlation functional. [127] We used the SZV basis set [119] for both Ti and O atoms to generate the localized states in a 3x3x5 supercell [a=13.869 Å, b=13.869 Å, c=14.907 Å], [α=90, β=90, γ=90]. The results obtained for different +U values on the ***3d*** atomic shell of Ti are shown in Table 6.

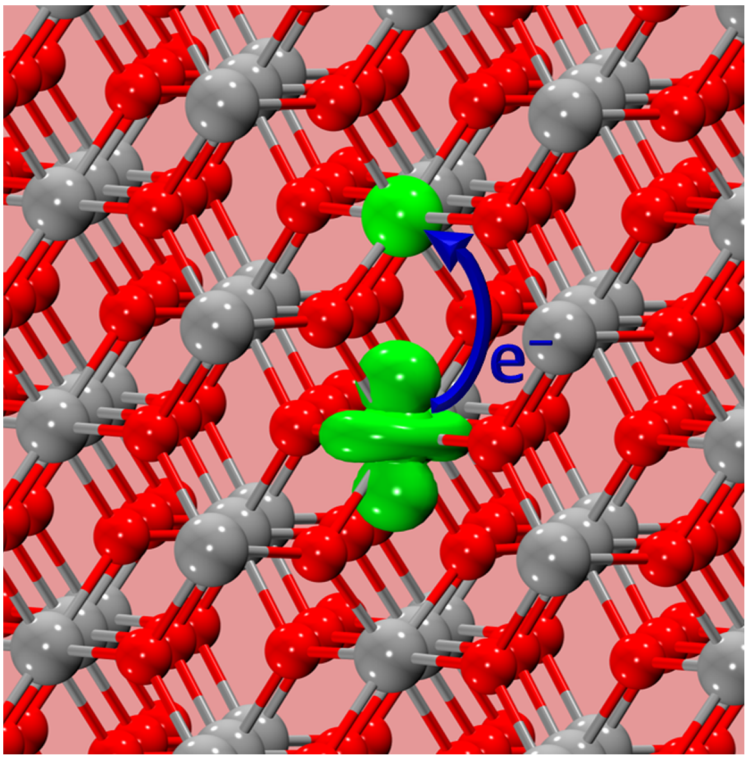

Figure 6. Rutile TiO_2 with an iso-surface of the spin density of an electron localized on a Ti atom. The hop between two Ti atoms is marked in blue color in the [001] direction. The silver spheres are Ti atoms, the red spheres are O atoms, green spheres are the polaronic Ti atoms.

Rutile TiO_2	U = 6 eV	U = 8 eV	U = 10 eV	ref. 119
ΔG* (eV)	0.269	0.275	0.280	0.288
λ/4 (eV)	0.263	0.274	0.281	0.288
$\boldsymbol{V_{AB}}$ (eV)	0.230	0.149	0.129	0.200
Adiabatic barrier (eV)	0.039	0.126	0.152	0.088
Overlap $\lvert S_{AB} \rvert$	0.061	0.003	0.017	

Table 6. V_{AB} for electron transfer in the c-direction for bulk TiO_2 from PBE+U orbitals. ΔG is the energy of the mid-point along the reaction pathway, λ is the reorganization energy, $\boldsymbol{V_{AB}}$ is the electronic coupling, and the adiabatic barrier is equal to (ΔG* - $\boldsymbol{V_{AB}}$).*

Deskins et al. [128] reported V_{AB} values of ~ 0.2 eV for a ***c***-direction hop from cluster calculations. Our calculated value is of the same order of magnitude. In particular, there is a good match between the λ reorganization energies.

3.f Bulk ms-$BiVO_4$

Our last test calculation involves V_{AB} calculation for an electron polaron transfer in bismuth vanadate $BiVO_4$ (BVO). BVO is a semiconductor that exhibit promising performance toward overall water splitting.[67] In previous work we characterized electron polaron and hole polaron transport in monoclinic ms-BVO, obtaining the reorganization energy with plane wave periodic PBE+U wavefunctions and V_{AB} with a small model cluster ***HF*** calculation.[67] Here our calculation was for an electron polaron transfer from a V atom to a nearest neighbor in the (021) direction in bulk BVO.

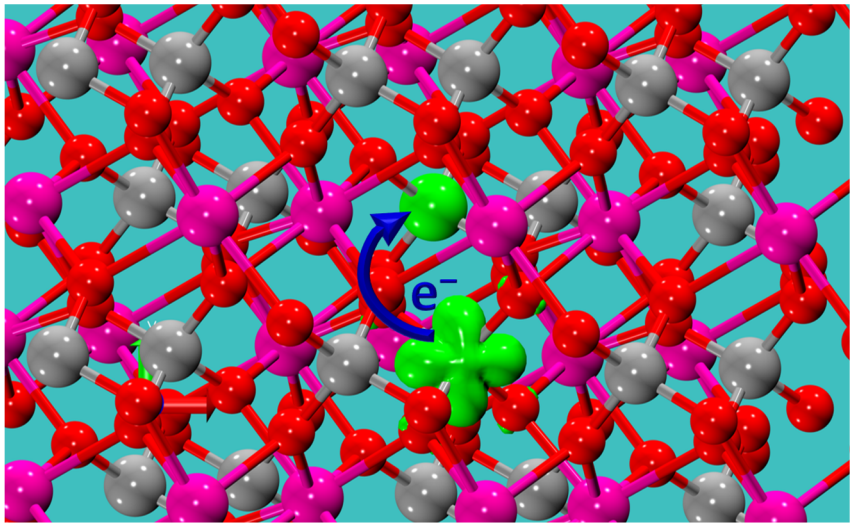

Figure 7. ms-BiVO4 with an iso-surface of spin density for an electron localized at a V atom. The hop between two V atoms is indicated in blue color. The green spheres are polaronic V atoms, silver spheres are V atoms, the red spheres are O atoms, and purple spheres are Bi atoms.

We used a DFT+U level of theory based on the PBE exchange correlation functional. [129] We used the SZV basis set[119] for both V and O atoms to generate the localized states in a 3x3x1 supercell [a=15.587 Å, b=15.281 Å, c=11.704 Å], [α=90, β=90, γ=90.383]. The results obtained for different +U values on the *3d* atomic states of V are shown in Table 7. The calculated values of V_{AB} and of the diabatic activation barrier are in good accord with our earlier work. In particular, V_{AB} is small.

$BiVO_4$	PBE+U U = 6 eV	PBE+U U = 8 eV
ΔG* (eV)	0.295	0.305
λ/4 (eV)	0.295	0.288
V_{AB} (eV)	0.010	0.040
Adiabatic barrier (eV)	0.285	0.265
Overlap $\lvert S_{AB} \rvert$	0.113	0.078

Table 7. V_{AB} for electron transfer in the (021) direction in bulk $BiVO_4$ from PBE+U orbitals. ΔG^* is the energy of the mid-point along the hopping pathway, λ is the reorganization energy, $\boldsymbol{V_{AB}}$ is the electronic coupling, and the adiabatic barrier is equal to ($\Delta G^* - \boldsymbol{V_{AB}}$).

4. Conclusions

In this paper we reported a new implementation of a method for the calculation of the electronic coupling matrix element $\boldsymbol{V_{AB}}$ of ET theory in periodic systems. We presented test calculations that highlight the capability of the new module that is embedded in the CP2K code, as described in the ***Appendix B.*** The capability allows the complete characterization of ET in the solid state via the two localized quasi-diabatic state Marcus/Holstein model of polaron. It can be used for any single determinant representation of the electronic structure of the system from ***HF***, ***DFT***, ***hybrid DFT***, ***DFT+U***, or ***cDFT*** theory. Results are given for a number of test systems including iron oxide models, hematite Fe_2O_3, titanium dioxide TiO_2, and bismuth vanadate $BiVO_4$. The computer code re-uses several of the high-performance computing functions of CP2K. The method requires only the equivalent of one iteration of an ***HF*** calculation. The ability to calculate $\boldsymbol{H_{AB}}$ for localized states allows the complete treatment of polaron transport in semiconductors at the periodic ***DFT*** level of theory.

5. Acknowledgements

PB gratefully acknowledges the guidance of Dr. Nina Tyminska in designing our early polaron calculations and in assisting with the pictorial representation of localized polarons. MD acknowledges many stimulating discussions with Prof. Jochen Blumberger. We dedicate this paper to Prof. Michiel Sprik for his seminal and stimulating contributions to theories, methods, developments, and studies of electron transfer in the condensed phase and of redox reactivity at solid-liquid interfaces. We gratefully acknowledge start-up funds from University at Buffalo, and support from the U.S. Department of Energy, Office of Science, Office of Basic Energy Sciences, under Award Number(s) DE-SC0019086. We thank Prof. Juerg Hutter and other participants on the CP2K user forum for assistance and guidance about the methods and their implementations in CP2K. We also acknowledge support from the Center for Computational Research at the University at Buffalo.

6. APPENDIX A: Considerations about localized states and V_{AB} calculations

The essential differences between several formalisms and implementations of ET lie in the nature of the quasi-diabatic ***n***-electron states $\boldsymbol{\Psi_A}$ and $\boldsymbol{\Psi_B}$ and in the expression used for the evaluation of the Hamiltonian elements $\boldsymbol{H_{AA}}$, $\boldsymbol{H_{BB}}$, and $\boldsymbol{H_{AB}}$. In the recent of work of Bylaska and Rosso[105] valid for molecular and periodic calculations, $\boldsymbol{\Psi_A}$ and $\boldsymbol{\Psi_B}$ are ***HF*** states, and ***H*** is the total ***n***-electron Hamiltonian, the evaluation of which introduces exact exchange terms requiring exact exchange integrals as in ***HF*** theory. In the work of Van Voorhis and collaborators [88] using ***cDFT***, the $\boldsymbol{\Psi_A}$ and $\boldsymbol{\Psi_B}$ ***n***-electron states are Kohn-Sham-like states for which constraints have been applied to enable charge or spin localization, and the Hamiltonian terms in eq.(1) are taken as the ***DFT*** Kohn-Sham Hamiltonian. Strictly speaking, the ***DFT*** Hamiltonian for ***A*** is not the same as the Hamiltonian for ***B*** since the ***DFT*** Hamiltonian is state-specific through the functional of the

density. As such the KS Hamiltonian depends on the electron density of state ***A*** or ***B*** respectively, albeit it is the case that $E_A^{KS} \equiv E_B^{KS}$ when the ET process is thermo-neutral.

If we denote ***H(1,2,…,n)*** the total ***n***-electron Hamiltonian operator, and ***H_A(1,2,…,n)*** and ***H_B(1,2,…, n)*** the Kohn-Sham operators for state ***A*** and state ***B*** respectively, it follows that:

$$H_A(1,2,\dots,n) \neq H(1,2,\dots,n)$$

$$H_B(1,2,\dots,n) \neq H(1,2,\dots,n)$$

$$E_A^{KS} = \langle \Psi_A^{KS} \big| H_A(1,2,\dots,n) \big| \Psi_A^{KS} \rangle \neq \langle \Psi_A^{KS} \big| H(1,2,\dots,n) \big| \Psi_A^{KS} \rangle$$

$$E_A^{KS} = \langle \Psi_B^{KS} | H_B(1,2,\dots,n) | \Psi_B^{KS} \rangle \neq \langle \Psi_B^{KS} | H(1,2,\dots,n) | \Psi_B^{KS} \rangle \qquad (A.1)$$

We can project the occupied Kohn-Sham (KS) ***1***-electron states onto the Hartree-Fock ***1***-electron states (occupied and unoccupied):

$$\begin{aligned} \left(\varphi_1^{KS,A}, \varphi_2^{KS,A}, \dots, \varphi_n^{KS,A}\right) &= \left(\varphi_1^{HF}, \varphi_2^{HF}, \dots, \varphi_n^{HF}\right) \times C_{(M,n)}^{A} \\ \left(\varphi_1^{KS,B}, \varphi_2^{KS,B}, \dots, \varphi_n^{KS,B}\right) &= \left(\varphi_1^{HF}, \varphi_2^{HF}, \dots, \varphi_n^{HF}\right) \times C_{(M,n)}^{B} \end{aligned} \qquad (A.2)$$

where the ***C's*** are ***M×n*** matrices, ***M*** is the total number of ***1***-electron ***HF*** states, and ***n*** is the number of ***1***-electron occupied ***KS*** states. It follows that we can expand the ***KS*** determinant as a linear combination of excited ***HF*** determinants, following Lowdin[130]:

$$\Psi^{KS} = c_0 \Psi^{HF} + \sum_{i}^{a} c_{i\to a} \Psi_{i\to a}^{HF} + \sum_{i,j}^{a,b} c_{i,j\to a,b} \Psi_{i,j\to a,b}^{HF} + \sum_{i,j,k}^{a,b,c} c_{i,j,k\to a,b,c} \Psi_{i,j,k\to a,b,c}^{HF} + \cdots \qquad (A.3)$$

In eq.(A.3) $\Psi_{i,a}^{HF}, \Psi_{i,j,a,b}^{HF}, \Psi_{i,j,k,a,b,c}^{HF}, \dots$ denote singly-, doubly-, triply-excited, … determinants where occupied orbital ***i, j, k,*** … have been replaced by unoccupied orbitals ***a, b, c,*** … . In effect we can expand the ***KS*** determinant as a configuration interaction (CI) expansion involving the ***HF*** determinant plus singly-excited determinants plus doubly-excited determinants plus … ***n***-excited determinants.[130] It emerges that a single determinant ***KS*** wavefunctions can be conceived as very compact representations of complex CI wavefunctions based on excited ***HF*** determinants. In particular, in our case, they have the desired character of representing 'localized' states, but in addition, they also capture a description of electron correlation that ***HF*** wavefunctions do not.

We can apply the variational principle to the two ***KS n***-electron states using the total ***n***-electron Hamiltonian to obtain the 'best' linear combination. This is what is expressed in eqs. (1 and 2).

$$\begin{aligned} \Psi_{\pm} &= c_{\pm}^{A} \Psi_A^{KS} + c_{\pm}^{B} \Psi_B^{KS} \\ H_{AA} &= \langle \Psi_A^{KS} | H(1,2\cdots n) | \Psi_A^{KS} \rangle \\ H_{BB} &= \langle \Psi_B^{KS} | H(1,2\cdots n) | \Psi_B^{KS} \rangle \\ H_{AB} &= \langle \Psi_A^{KS} | H(1,2\cdots n) | \Psi_B^{KS} \rangle \end{aligned} \qquad (A.4)$$

The diagonal terms in the secular equation in eq. (2) of the main text are now the 'exact' energies associated with the ***KS*** determinants (using the exact ***n***-electron Hamiltonian). The off-diagonal terms can be calculated through the usual formalism of the "corresponding orbital transformation"

(COT) that is a bi-orthogonalization procedure applicable to spin-polarized states as described below. Lastly, we note that Marcus/Holstein theory does not tell us how to build the quasi-diabatic states: we may use "localized" ***HF*** states, "localized" ***DFT*** states, "***DFT+U***" states, "hybrid ***DFT***" states, or "constrained ***DFT***" states. The formalism is applicable to molecular systems as well as periodic systems, and the computational cost for the calculation of $\boldsymbol{V_{AB}}$ is equivalent to one iteration of a ***HF*** calculation.

7. APPENDIX B: CP2K implementation details

In this Appendix, we gather for convenience the essential equations embodied in CP2K that are relevant to the calculation of $\boldsymbol{V_{AB}}$ developed here. CP2K implements a mixed Gaussian and plane wave method to perform efficient *ab initio* calculations.[111,117,131-138] CP2K is highly parallel and scales linearly with the system size even for condensed phase systems. The essential feature of the Gaussian and plane wave approach is the dual representation of the electron density that allows an efficient treatment of electrostatics. We implemented our calculation of $\boldsymbol{V_{AB}}$ within the GAPW (Gaussian augmented plane wave) and GPW(Gaussian Plane Wave) formalisms of CP2K [131,132] making use of many routines available in CP2K, [111,134] in particular the Coulomb engine and the exchange engine. The re-use of subroutines was made possible because of the decomposition of the generalized density matrix in the $\boldsymbol{V_{AB}}$ calculation into a symmetric component and an anti-symmetric component.

The expression for the total energy of a molecular or crystalline system in the GPW[133] formalism is as follows:

$$\begin{aligned} E_{Total} &= E^T[n] + E^V[n] + E^H[n] + E^X[n] + E^{Ion-Ion} \\ &= \sum_{\mu\nu} P_{\mu\nu} \langle \varphi_\mu(\boldsymbol{r}) \left| -\frac{\Delta}{2} \right| \varphi_\nu(\boldsymbol{r}) \rangle \\ &+ \sum_{\mu\nu} P_{\mu\nu} \langle \varphi_\mu(\boldsymbol{r}) | V_{nl}^{PP}(\boldsymbol{r},\boldsymbol{r}') | \varphi_\nu(\boldsymbol{r}) \rangle + \sum_{\mu\nu} P_{\mu\nu} \langle \varphi_\mu(\boldsymbol{r}) | V_{loc}^{PP}(\boldsymbol{r},\boldsymbol{r}') | \varphi_\nu(\boldsymbol{r}) \rangle \qquad (B.1) \\ &+ 4\pi\Omega \sum_{|\boldsymbol{G}|<G_C} \frac{\check{n}^*(\boldsymbol{G})\check{n}(\boldsymbol{G})}{\boldsymbol{G}^2} + E_{HFX} + \frac{1}{2}\sum_{I\neq J} \frac{Z_I - Z_J}{|\boldsymbol{R}_I - \boldsymbol{R}_J|} \end{aligned}$$

where $\boldsymbol{n}$ denotes the electron density, T is the electronic kinetic energy, V is the electronic potential energy, H is the Hartree energy, X is the exchange energy (exchange correlation in case of DFT), and PP stands for pseudo-potential.

The use of pseudo-potentials is a well-established technique to represent the nuclei and core electrons. They have local and non-local parts. The long-range contribution to the local part of pseudo-potentials to the energy, the Hartree energy, and the ion-ion nuclear interaction energy are grouped together as electrostatic interactions. They are treated via Ewald sum on a FFT grid. The short range part of the local pseudopotentials is treated on a real grid.

$$E_{electrostatic} = \int V_{loc}^{PP}(r)n(\boldsymbol{r})d\boldsymbol{r} + 4\pi\Omega \sum_{|\boldsymbol{G}|<G_C} \frac{\check{n}^*(\boldsymbol{G})\check{n}(\boldsymbol{G})}{\boldsymbol{G}^2} + \frac{1}{2}\sum_{I\neq J} \frac{Z_I - Z_J}{|\boldsymbol{R}_I - \boldsymbol{R}_J|} \quad (B.2)$$

For computational convenience a Gaussian core charge is introduced for each nucleus so that the above expression becomes:

$$E_{electrostatic} = \int V_{loc}^{SR}(r)n(\boldsymbol{r})d\boldsymbol{r} + \frac{\Omega}{2}\sum_{\boldsymbol{G}} \tilde{n}_{tot}^*(\boldsymbol{G}) \frac{4\pi\tilde{n}_{tot}(\boldsymbol{G})}{\boldsymbol{G^2}} + \frac{1}{2}\sum_{I\neq J} \frac{Z_I Z_J}{|\boldsymbol{R}_I - \boldsymbol{R}_J|} \operatorname{erfc}\left[\frac{|\boldsymbol{R}_I - \boldsymbol{R}_J|}{\sqrt{R_I^{c\,2} + R_J^{c\,2}}}\right] - \sum_I \frac{1}{\sqrt{2\pi}} \frac{Z_I^2}{R_I^c} \quad (B.3)$$

The last three terms are the total Hartree energy (E^H), the 'nuclear overlap' energy (E^{ovrl}), and the self-energy (E^{self}). The electron density in GAPW is treated differently as compared to GPW. It is divided into three parts, a smooth global density distributed over the whole space, and two non-overlapping atom centered soft and hard densities. These densities are constructed such that, within the region around the atoms, the soft density cancels the all-inclusive smooth density, and in the interstitial regions, soft and hard densities cancel out.

$$\begin{aligned} n &= \tilde{n} - \tilde{n}^1 + n^1 \\ n^1 &= \textstyle\sum_A n_A^1 \\ \tilde{n}^1 &= \displaystyle\sum_A \tilde{n}_A^1 \end{aligned} \quad (B.4)$$

where, n = electron density, $\tilde{n}$ = smooth global density, $\tilde{n}^1$=atom-centered soft density, and n^1=atom-centered hard density. More details on the construction of densities can be found in Lippert *et al.*[131,132] The Hartree energy term is computed in two parts, one with the smooth global density using a poisson solver on FFT grids, and the second part on an atomic Lebedev grid (spherical grid) with the atom-centered densities. Therefore

$$E_H[n + n^Z] = E_H[\tilde{n} + \tilde{n}^0] + \sum_A E_H[n_A^1 + n_A^Z] + \sum_A E_H[\tilde{n}_A^1 + n_A^0] + E_H[n^0] - E_H[\tilde{n}^0] + \int d\boldsymbol{r}\, V_H[n^0 - \tilde{n}^0]\tilde{n} \quad (B.5)$$

where, the operators E_H and V_H are:

$$E_H[n] = \frac{1}{2}\iint d\boldsymbol{r}\, d\boldsymbol{r}' \frac{n(\boldsymbol{r})\, n(\boldsymbol{r}')}{|\boldsymbol{r} - \boldsymbol{r}'|} \quad (B.6)$$

$$V_H[n](\boldsymbol{r}) = \int d\boldsymbol{r}' \frac{n(\boldsymbol{r}')}{|\boldsymbol{r} - \boldsymbol{r}'|}$$

The ***HF*** Exchange energy calculation is calculated for the Γ-point only for periodic systems in CP2K, and makes use of a truncated coulomb operator using Gaussian basis sets. Implementation details can be found in papers by Guidon, et al.[111,134,139]

$$E_x^{PBC} = -\frac{1}{2N_k}\sum_{i,j}\sum_{\boldsymbol{k},\boldsymbol{k'}}\iint \psi_i^{\boldsymbol{k}}(r_1)\psi_j^{\boldsymbol{k'}}(r_1)g(|r_1-r_2|)\psi_i^{\boldsymbol{k}}(r_2)\psi_j^{\boldsymbol{k'}}(r_2)\, d^3r_1\, d^3r_2 \qquad (B.7)$$

For the purpose of our $\boldsymbol{V_{AB}}$ calculation, we needed to separate $\boldsymbol{H_{AB}}$ into: 1/ two-electron contributions - coulomb (or Hartree) and exchange; 2/ one-electron contributions - nuclear attraction and kinetic energy; and 3/ nuclear energy (ion-ion). The three contributions to the energies (Coloumb, ion-ion, and nuclear attraction) were obtained by three successive calls to the Poisson solver, the first time providing the electron density only, the second time providing the nuclear density only, and the third time providing the total density. Subtraction of the electron-only and nuclear-only energies, from the energy obtained with the combined density, yielded the one-electron contribution. We note that a part of the nuclear-only energy term cancels out a term in the pseudopotential contribution and hence the nuclear-only energy is equal to the pure nuclear energy only in cases of all-electron calculations. A similar procedure was applied to the one-center Hartree energy terms. The HFX routine provides the two-electron exchange energy. In the end the various energy contributions were gathered as shown in Table B1.

	1	2	3
Energy contributions	elec-elec	nuc-nuc	nuc-elec, kinetic energy
Associated CP2K function calls	2e- energies	0e- energies	1e- energies
Exchange: hfx_ks_matrix()	symmetric and anti-symmetric parts	-	-
E_Hartree: pw_poisson_solve()	call with electron-only density	call with nuclear-only density	Regular call with combined (1 + 2) density
E_Hartree_1centered: Vh_1c_gg_integrals()	call with electron-only density	call with nuclear-only density	Regular call with combined (1 + 2) density
Self-energy: calculate_ecore_self()	-	Analytical term	-
Potential energy: build_core_hamiltonian_matrix()	-	-	from core Hamiltonian
Kinetic energy: build_core_hamiltonian_matrix()	-	-	from core Hamiltonian
Summation by column gives:	Coulomb + Exchange energy	Ion-ion interaction energy	Ion-electron attraction energy

Table B1. Outline of one-electron, two-electron, and nuclear energy contributions obtained by splitting the subroutine calls within the 'quick-step' code and its construction of the Kohn-Sham matrix in CP2K.

When using the GPW formalism, there are no 1-centered Hartree energy terms. GAPW requires much care and tuning of parameters on a case-by-case basis, so that for periodic calculations it may be preferable to use the GPW method. GAPW and GPW results come out to be the same for $\boldsymbol{V_{AB}}$ calculations. For all-electron calculations the GAPW method is necessary. Convergence with respect to the radial atomic grids and the FFT grid must be checked to get accurate values of V_{AB}.

For the calculation of $\boldsymbol{V_{AB}}$, the COT method requires the orbitals of both initial and final states. For the sake of convenience, this is done in CP2K in a mixed energy calculation setup so that both states are available in the quick-step force environment at the same time. Generating the two localized states in itself require making use of broken symmetry section in CP2K, or Hubbard U, or constrained DFT, which are not discussed here. Using the generalized density matrix obtained from the initial and final state orbitals, a single step of ***HF*** energy calculation is carried out to obtain the segregated one-electron and two-electron contributions as shown in table 1.

We make use of the partitioning of the generalized density matrix into a symmetric matrix and an anti-symmetric matrix. For the Coulomb and one-electron terms the symmetric part of the generalized density matrix suffices as the operators are symmetric. However, for the calculation of exchange energy, both parts are needed and two 'exchange' calculations are carried out by passing symmetric and anti-symmetric matrices. The two contributions are summed up in the end. When using DFT-based states as initial and final states (non-HF orbitals) as input, then the theory developed above requires that we calculate the exact HF energy $\boldsymbol{H_{AA}}$ and $\boldsymbol{H_{BB}}$ (these quantities are already available if initial and final states are ***HF*** states). Finally, we assemble $\boldsymbol{V_{AB}}$ by multiplying the energy contributions with the appropriate pre-factors.

The code is implemented within a fork of publicly available CP2K-6.1 version. An input section "&VAB" provides the ***HF*** calculation parameters required during the $\boldsymbol{V_{AB}}$ calculation in cases when the orbitals are not ***HF*** orbitals. CP2K's object oriented design helps in replicating the ***HF*** options under the $\boldsymbol{V_{AB}}$ section. The input section is placed as part of the '**mixed**' section as illustrated below:

```
=========================================
&FORCE_EVAL
&MIXED
...
    &VAB
        DO_VAB .TRUE.
        &HF
           FRACTION 1.0  !Must be 1.0
            !Other optional sections for setting up HF calculation as in
            !Guidon, et al.'s papers on HF implementation in CP2K [111,134,139]
            !HF_INFO
            !INTERACTION_POTENTIAL
            !LOAD_BALANCE
            !MEMORY
            !PERIODIC
```

```
            !SCREENING
        &END
    &END
...
&END
&END

========================================
```

8. Conflicts of interest

There are no conflicts of interest to declare

9. Supplementary Information

The supporting information includes:

1. Modified basis sets used in helium dimer and iron oxide calculations.
2. Neutral geometries of systems
3. Source code and inputs for test cases are available at https://github.com/pavankum/cp2k-vab.

10. References

(1) Hush, N. S.; Vlcek, A. A.; Stranks, D. R.; Marcus, R. A.; Weiss, J.; Bell, R. P.; Halpern, J.; Orgel, L. E.; Adamson, A. W.; Dainton, F. S.; Williams, R. J. P.; Taube, H.; Shimi, I. A. W.; Higginson, W. C. E.; Stead, J. B.; Waind, G. M.; Rosseinsky, D. R.; Wells, C. F.; Sutcliffe, L. H.; Proll, P. J.; King, E. L.; Stranks, D. R.; Pearson, R. G.; Basolo, F.; Poe, A. J.; Fordsmith, M. H.; Sutin, N.; Dodson, R. W.; Baughan, C. Exchange reactions and electron transfer reactions including isotopic exchange - general discussion. *Discussions of the Faraday Society* **1960**, 113-136.

(2) Marcus, R. A. Theory of oxidation-reduction reactions involving electron transfer .4. A statistical-mechanical basis for treating contributions from solvent, ligands, and inert salt. *Discussions of the Faraday Society* **1960**, 21-31.

(3) Marcus, R. A. Chemical + electrochemical electron-transfer theory. *Annual Review of Physical Chemistry* **1964**, *15*, 155-196.

(4) Marcus, R. A. On theory of electron-transfer reactions .6. Unified treatment for homogeneous and electrode reactions. *Journal of Chemical Physics* **1965**, *43*, 679.

(5) Marcus, R. A. Electron transfer at electrodes and in solution - comparison of theory and experiment. *Electrochimica Acta* **1968**, *13*, 995-&.

(6) Marcus, R. A.; Siders, P. Further developments in electron-transfer. *Acs Symposium Series* **1982**, *198*, 235-253.

(7) Marcus, R. A.; Sutin, N. Electron Transfers in Chemistry and Biology. *Biochimica Et Biophysica Acta* **1985**, *811*, 265-322.

(8) Marcus, R. A. Electron-transfer reactions in chemistry - Theory and experiment. *Reviews of Modern Physics* **1993**, *65*, 599-610.

(9) Warshel, A. Dynamics of reactions in polar-solvents - semi-classical trajectory studies of electron-transfer and proton-transfer reactions. *Journal of Physical Chemistry* **1982**, *86*, 2218-2224.

(10) Hwang, J. K.; Warshel, A. Microscopic examination of free-energy relationships for electron-transfer in polar-solvents. *Journal of the American Chemical Society* **1987**, *109*, 715-720.

(11) King, G.; Warshel, A. Investigation of the free-energy functions for electron-transfer reactions. *Journal of Chemical Physics* **1990**, *93*, 8682-8692.

(12) Kuharski, R. A.; Bader, J. S.; Chandler, D.; Sprik, M.; Klein, M. L.; Impey, R. W. Molecular-model for aqueous ferrous ferric electron-transfer. *Journal of Chemical Physics* **1988**, *89*, 3248-3257.

(13) Logan, J.; Newton, M. D. Abinitio study of electronic coupling in the aqueous Fe-2+-Fe-3+ electron exchange process. *Journal of Chemical Physics* **1983**, *78*, 4086-4091.

(14) Newton, M. D.; Sutin, N. Electron-transfer reactions in condensed phases. *Annual Review of Physical Chemistry* **1984**, *35*, 437-480.

(15) Newton, M. D. Electronic-structure analysis of electron-transfer matrix-elements for transition-metal redox pairs. *Journal of Physical Chemistry* **1988**, *92*, 3049-3056.

(16) Blumberger, J.; Sprik, M. Free energy of oxidation of metal aqua ions by an enforced change of coordination. *Journal of Physical Chemistry B* **2004**, *108*, 6529-6535.

(17) Blumberger, J.; Sprik, M. Ab initio molecular dynamics simulation of the aqueous Ru2+/Ru3+ redox reaction: The Marcus perspective. *Journal of Physical Chemistry B* **2005**, *109*, 6793-6804.

(18) Blumberger, J.; Sprik, M. Quantum versus classical electron transfer energy as reaction coordinate for the aqueous Ru2+/Ru3+ redox reaction. *Theoretical Chemistry Accounts* **2006**, *115*, 113-126.

(19) Barbara, P. F.; Meyer, T. J.; Ratner, M. A. Contemporary Issues in Electron Transfer Research. *The Journal of Physical Chemistry* **1996**, *100*, 13148-13168.

(20) Blumberger, J. Recent Advances in the Theory and Molecular Simulation of Biological Electron Transfer Reactions. *Chemical Reviews* **2015**, *115*, 11191-11238.

(21) Beratan, D. N.; Skourtis, S. S.; Balabin, I. A.; Balaeff, A.; Keinan, S.; Venkatramani, R.; Xiao, D. Q. Steering Electrons on Moving Pathways. *Accounts of Chemical Research* **2009**, *42*, 1669-1678.

(22) Beratan, D. N.: Why Are DNA and Protein Electron Transfer So Different? In *Annual Review of Physical Chemistry, Vol 70*; Johnson, M. A., Martinez, T. J., Eds.; Annual Review of Physical Chemistry, 2019; Vol. 70; pp 71-97.

(23) Friedman, L.; Holstein, T. Studies of polaron motion .3. the hall mobility of the small polaron. *Annals of Physics* **1963**, *21*, 494-549.

(24) Emin, D.; Holstein, T. Adiabatic Theory of Hall Mobility of Small Polaron in Hopping Regime. *Bulletin of the American Physical Society* **1968**, *13*, 464.

(25) Emin, D.; Holstein, T. Studies of Small Polaron Motion. 4. Adiabatic Theory of Hall Effects. *Annals of Physics* **1969**, *53*, 439-520.

(26) Austin, I. G.; Mott, N. F. Polarons in Crystalline and Non-Crystalline Materials. *Advances in Physics* **1969**, *18*, 41-102.

(27) Emin, D. Correlated small-polaron hopping motion. *Physical Review Letters* **1970**, *25*, 1751-1755.

(28) Emin, D. Lattice Relaxation and Small-Polaron Hopping Motion. *Physical Review B* **1971**, *4*, 3639-3651.

(29) Emin, D. Phonon-assisted transition rates .1. optical-phonon-assisted hopping in solids. *Advances in Physics* **1975**, *24*, 305-348.

(30) Emin, D. Transport properties of small polarons. *Journal of Solid State Chemistry* **1975**, *12*, 246-252.

(31) Iordanova, N.; Dupuis, M.; Rosso, K. M. Charge transport in metal oxides: A theoretical study of hematite alpha-Fe2O3. *Journal of Chemical Physics* **2005**, *122*, 144305.

(32) Deskins, N. A.; Dupuis, M. Electron transport via polaron hopping in bulk TiO2: A density functional theory characterization. *Physical Review B* **2007**, *75*, 195212-195221.

(33) Deskins, N. A.; Rao, P. M.; Dupuis, M. Charge carrier management in semiconductors: mdodelng charge transport and recombination. *Springer Handbook of Inorganic Photochemistry* **2019**.

(34) Oberhofer, H.; Reuter, K.; Blumberger, J. Charge Transport in Molecular Materials: An Assessment of Computational Methods. *Chemical Reviews* **2017**, *117*, 10319-10357.

(35) Shirakawa, H.; Louis, E. J.; Macdiarmid, A. G.; Chiang, C. K.; Heeger, A. J. Synthesis of electrically conducting organic polymers - halogen derivatives of polyacetylene, (CH)x. *Journal of the Chemical Society-Chemical Communications* **1977**, 578-580.

(36) Chiang, C. K.; Fincher, C. R.; Park, Y. W.; Heeger, A. J.; Shirakawa, H.; Louis, E. J.; Gau, S. C.; Macdiarmid, A. G. Electrical-conductivity in doped polyacetylene. *Physical Review Letters* **1977**, *39*, 1098-1101.

(37) Chiang, C. K.; Park, Y. W.; Heeger, A. J.; Shirakawa, H.; Louis, E. J.; Macdiarmid, A. G. Conducting polymers - halogen doped polyacetylene. *Journal of Chemical Physics* **1978**, *69*, 5098-5104.

(38) Ikehata, S.; Kaufer, J.; Woerner, T.; Pron, A.; Druy, M. A.; Sivak, A.; Heeger, A. J.; Macdiarmid, A. G. Solitons in polyacetylene - magnetic-susceptibility. *Physical Review Letters* **1980**, *45*, 1123-1126.

(39) Park, Y. W.; Heeger, A. J.; Druy, M. A.; Macdiarmid, A. G. Electrical transport in doped polyacetylene. *Journal of Chemical Physics* **1980**, *73*, 946-957.

(40) Chen, S. N.; Heeger, A. J.; Kiss, Z.; Macdiarmid, A. G.; Gau, S. C.; Peebles, D. L. Polyacetylene, (CH)x - photoelectrochemical solar-cell. *Applied Physics Letters* **1980**, *36*, 96-98.

(41) Etemad, S.; Mitani, T.; Ozaki, M.; Chung, T. C.; Heeger, A. J.; Macdiarmid, A. G. Photoconductivity in polyacetylene. *Solid State Communications* **1981**, *40*, 75-79.

(42) Heeger, A. J.; Macdiarmid, A. G. Transport, magnetic and structural studies of polyacetylene. *Molecular Crystals and Liquid Crystals* **1981**, *77*, 1-24.

(43) Moses, D.; Chen, J.; Denenstein, A.; Kaveh, M.; Chung, T. C.; Heeger, A. J.; Macdiarmid, A. G.; Park, Y. W. Inter-soliton electron hopping transport in trans-(CH)x. *Solid State Communications* **1981**, *40*, 1007-1010.

(44) Su, W. P.; Schrieffer, J. R.; Heeger, A. J. Solitons in polyacetylene. *Physical Review Letters* **1979**, *42*, 1698-1701.

(45) Su, W. P.; Schrieffer, J. R.; Heeger, A. J. Soliton excitations in polyacetylene. *Physical Review B* **1980**, *22*, 2099-2111.

(46) Bredas, J. L.; Chance, R. R.; Silbey, R. Theoretical-studies of charged defect states in doped polyacetylene and polyparaphenylene. *Molecular Crystals and Liquid Crystals* **1981**, *77*, 319-332.

(47) Bredas, J. L.; Street, G. B. Polarons, Bipolarons, and Solitons in Conducting Polymers. *Accounts of Chemical Research* **1985**, *18*, 309-315.

(48) Bredas, J. L.; Calbert, J. P.; da Silva, D. A.; Cornil, J. Organic semiconductors: A theoretical characterization of the basic parameters governing charge transport. *Proceedings of the National Academy of Sciences of the United States of America* **2002**, *99*, 5804-5809.

(49) Bredas, J. L.; Beljonne, D.; Coropceanu, V.; Cornil, J. Charge-transfer and energy-transfer processes in pi-conjugated oligomers and polymers: A molecular picture. *Chemical Reviews* **2004**, *104*, 4971-5003.

(50) Coropceanu, V.; Cornil, J.; da Silva, D. A.; Olivier, Y.; Silbey, R.; Bredas, J. L. Charge transport in organic semiconductors. *Chemical Reviews* **2007**, *107*, 926-952.

(51) Bredas, J. L.; Norton, J. E.; Cornil, J.; Coropceanu, V. Molecular Understanding of Organic Solar Cells: The Challenges. *Accounts of Chemical Research* **2009**, *42*, 1691-1699.

(52) Kippelen, B.; Bredas, J. L. Organic photovoltaics. *Energy & Environmental Science* **2009**, *2*, 251-261.

(53) Korzdorfer, T.; Bredas, J. L. Organic Electronic Materials: Recent Advances in the DFT Description of the Ground and Excited States Using Tuned Range-Separated Hybrid Functionals. *Accounts of Chemical Research* **2014**, *47*, 3284-3291.

(54) Rosso, K. M.; Dupuis, M. On charge transport in iron oxides. *Geochimica Et Cosmochimica Acta* **2005**, *69*, A778-A778.

(55) Kerisit, S.; Rosso, K. M. Kinetic Monte Carlo model of charge transport in hematite (alpha-Fe2O3). *Journal of Chemical Physics* **2007**, *127*, 124706-124715.

(56) Skomurski, F. N.; Kerisit, S.; Rosso, K. M. Structure, charge distribution, and electron hopping dynamics in magnetite (Fe3O4) (100) surfaces from first principles. *Geochimica Et Cosmochimica Acta* **2010**, *74*, 4234-4248.

(57) Katz, J. E.; Zhang, X. Y.; Attenkofer, K.; Chapman, K. W.; Frandsen, C.; Zarzycki, P.; Rosso, K. M.; Falcone, R. W.; Waychunas, G. A.; Gilbert, B. Electron Small Polarons and Their Mobility in Iron (Oxyhydr)oxide Nanoparticles. *Science* **2012**, *337*, 1200-1203.

(58) Yu, J. G.; Rosso, K. M.; Bruemmer, S. M. Charge and Ion Transport in NiO and Aspects of Ni Oxidation from First Principles. *Journal of Physical Chemistry C* **2012**, *116*, 1948-1954.

(59) Alexandrov, V.; Rosso, K. M. Electron transport in pure and substituted iron oxyhydroxides by small-polaron migration. *Journal of Chemical Physics* **2014**, *140*, 234701-234708.

(60) Alexandrov, V.; Rosso, K. M. Ab initio modeling of Fe(II) adsorption and interfacial electron transfer at goethite (alpha-FeOOH) surfaces. *Physical Chemistry Chemical Physics* **2015**, *17*, 14518-14531.

(61) Chatman, S.; Zarzycki, P.; Rosso, K. M. Spontaneous Water Oxidation at Hematite (alpha-Fe2O3) Crystal Faces. *Acs Applied Materials & Interfaces* **2015**, *7*, 1550-1559.

(62) Kerisit, S.; Zarzycki, P.; Rosso, K. M. Computational Molecular Simulation of the Oxidative Adsorption of Ferrous Iron at the Hematite (001)-Water Interface. *Journal of Physical Chemistry C* **2015**, *119*, 9242-9252.

(63) Zarzycki, P.; Kerisit, S.; Rosso, K. M. Molecular Dynamics Study of Fe(II) Adsorption, Electron Exchange, and Mobility at Goethite (alpha-FeOOH) Surfaces. *Journal of Physical Chemistry C* **2015**, *119*, 3111-3123.

(64) Deskins, N. A.; Dupuis, M. Intrinsic Hole Migration Rates in TiO2 from Density Functional Theory. *Journal of Physical Chemistry C* **2009**, *113*, 346-358.

(65) Morbec, J. M.; Galli, G. Charge transport properties of bulk Ta3N5from first principles. *Physical Review B* **2016**, *93*, 035201-035206.

(66) Plata, J. J.; Marquez, A. M.; Sanz, J. F. Electron Mobility via Polaron Hopping in Bulk Ceria: A First-Principles Study. *Journal of Physical Chemistry C* **2013**, *117*, 14502-14509.

(67) Liu, T.; Pasumarthi, V.; LaPorte, C.; Feng, Z.; Li, Q.; Yang, J.; Li, C.; Dupuis, M. Bimodal hole transport in bulk BiVO4 from computation. *Journal of Materials Chemistry* **2018**, *6*, 3714-3723.

(68) Pasumarthi, V.; Liu, T.; Dupuis, M.; Li, C. Charge carrier transport dynamics in W/Mo-doped BiVO4 : first principles-based mesoscale characterization. *Journal of Materials Chemistry A.* **2019**, *7*, 3054-3065.

(69) Liao, P. L.; Carter, E. A. Optical Excitations in Hematite (alpha-Fe2O3) via Embedded Cluster Models: A CASPT2 Study. *Journal of Physical Chemistry C* **2011**, *115*, 20795-20805.

(70) Liao, P. L.; Toroker, M. C.; Carter, E. A. Electron Transport in Pure and Doped Hematite. *Nano Letters* **2011**, *11*, 1775-1781.

(71) Toroker, M. C.; Carter, E. A. Hole Transport in Nonstoichiometric and Doped Wustite. *Journal of Physical Chemistry C* **2012**, *116*, 17403-17413.

(72) Kanan, D. K.; Carter, E. A. Ab initio study of electron and hole transport in pure and doped MnO and MnO:ZnO alloy. *Journal of Materials Chemistry A* **2013**, *1*, 9246-9256.

(73) Newton, M. D. Formalisms for electron-exchange kinetics in aqueous solution and the role of ab initio technqiues in their implementation. *International Journal of Quantum Chemistry* **1980**, *17*, 363-391.

(74) Leontyev, I. V.; Basilevsky, M. V.; Newton, M. D. Theory and computation of electron transfer reorganization energies with continuum and molecular solvent models. *Theoretical Chemistry Accounts* **2004**, *111*, 110-121.

(75) Cave, R. J.; Newton, M. D. Generalization of the Mulliken-Hush treatment for the calculation of electron transfer matrix elements. *Chemical Physics Letters* **1996**, *249*, 15-19.

(76) Cave, R. J.; Newton, M. D. Calculation of electronic coupling matrix elements for ground and excited state electron transfer reactions: Comparison of the generalized Mulliken-Hush and block diagonalization methods. *Journal of Chemical Physics* **1997**, *106*, 9213-9226.

(77) Cave, R. J.; Newton, M. D. Multistate Treatments of the Electronic Coupling in Donor-Bridge-Acceptor Systems: Insights and Caveats from a Simple Model. *Journal of Physical Chemistry A* **2014**, *118*, 7221-7234.

(78) Cave, R. J.; Edwards, S. T.; Kouzelos, J. A.; Newton, M. D. Reduced Electronic Spaces for Modeling Donor/Acceptor Interactions. *Journal of Physical Chemistry B* **2010**, *114*, 14631-14641.

(79) Ohta, K.; Closs, G. L.; Morokuma, K.; Green, N. J. Stereoelectronic effects in intramolecular long-distance electron-transfer in radical-anions as predicted by *ab initio* MO calculations. *Journal of the American Chemical Society* **1986**, *108*, 1319-1320.

(80) Farazdel, A.; Dupuis, M.; Clementi, E.; Aviram, A. Electric-Field Induced Intramolecular Electron Transfer in Spiro pi-Electron Systems and Their Suitability as Molecular Electronic Devices - A Theoretical Study. *Journal of the American Chemical Society* **1990**, *112*, 4206-4214.

(81) Jordan, K. D.; Paddonrow, M. N. Analysis of the interactions responsible for long-range through-bond-mediated electronic coupling between remote chromophores attached to rigid polynorbornyl bridges. *Chemical Reviews* **1992**, *92*, 395-410.

(82) Shephard, M. J.; Paddonrow, M. N.; Jordan, K. D. Electronic coupling through saturated-hydrocarbon bridges. *Chemical Physics* **1993**, *176*, 289-304.

(83) Paddon-Row, M. N. Investigating lang-range electron transfer processes with rigid, covalently linked donor-(norbornylogous bridge)-acceptor systems. *Accounts of Chemical Research* **1994**, *27*, 18-25.

(84) Hohenberg, P.; Kohn, W. Inhomogeneous electron gas. *Physical Reviews* **1964**, *136*, B864-B871.

(85) Kohn, W.; Sham, L. J. Self-consistent equations including exchange and correlation effects. *Physical Review* **1965**, *140*, 1133-&.

(86) Kaduk, B.; Kowalczyk, T.; Van Voorhis, T. Constrained Density Functional Theory. *Chemical Reviews* **2012**, *112*, 321-370.

(87) Wu, Q.; Van Voorhis, T. Constrained density functional theory and its application in long-range electron transfer. *Journal of Chemical Theory and Computation* **2006**, *2*, 765-774.

(88) Wu, Q.; Van Voorhis, T. Extracting electron transfer coupling elements from constrained density functional theory. *Journal of Chemical Physics* **2006**, *125*.

(89) Ding, F. Z.; Wang, H. B.; Wu, Q.; Van Voorhis, T.; Chen, S. W.; Konopelski, J. P. Computational Study of Bridge-Assisted Intervalence Electron Transfer. *Journal of Physical Chemistry A* **2010**, *114*, 6039-6046.

(90) Difley, S.; Van Voorhis, T. Exciton/Charge-Transfer Electronic Couplings in Organic Semiconductors. *Journal of Chemical Theory and Computation* **2011**, *7*, 594-601.

(91) Goldey, M. B.; Brawand, N. P.; Voros, M.; Galli, G. Charge Transport in Nanostructured Materials: Implementation and Verification of Constrained Density Functional Theory. *Journal of Chemical Theory and Computation* **2017**, *13*, 2581-2590.

(92) Futera, Z.; Blumberger, J. Electronic Couplings for Charge Transfer across Molecule/Metal and Molecule/Semiconductor Interfaces: Performance of the Projector Operator-Based Diabatization Approach. *Journal of Physical Chemistry C* **2017**, *121*, 19677-19689.

(93) Gillet, N.; Berstis, L.; Wu, X. J.; Gajdos, F.; Heck, A.; de la Lande, A.; Blumberger, J.; Elstner, M. Electronic Coupling Calculations for Bridge-Mediated Charge Transfer Using Constrained Density Functional Theory (CDFT) and Effective Hamiltonian Approaches at the Density Functional Theory (DFT) and Fragment-Orbital Density Functional Tight Binding (FODFTB) Level. *Journal of Chemical Theory and Computation* **2016**, *12*, 4793-4805.

(94) Kubas, A.; Gajdos, F.; Heck, A.; Oberhofer, H.; Elstner, M.; Blumberger, J. Electronic couplings for molecular charge transfer: benchmarking CDFT, FODFT and FODFTB against high-level ab initio calculations. II. *Physical Chemistry Chemical Physics* **2015**, *17*, 14342-14354.

(95) Kubas, A.; Hoffmann, F.; Heck, A.; Oberhofer, H.; Elstner, M.; Blumberger, J. Electronic couplings for molecular charge transfer: Benchmarking CDFT, FODFT, and FODFTB against high-level ab initio calculations. *Journal of Chemical Physics* **2014**, *140*.

(96) Manna, D.; Blumberger, J.; Martin, J. M. L.; Kronik, L. Prediction of electronic couplings for molecular charge transfer using optimally tuned range-separated hybrid functionals. *Molecular Physics* **2018**, *116*, 2497-2505.

(97) Oberhofer, H.; Blumberger, J. Charge constrained density functional molecular dynamics for simulation of condensed phase electron transfer reactions. *Journal of Chemical Physics* **2009**, *131*.

(98) Oberhofer, H.; Blumberger, J. Electronic coupling matrix elements from charge constrained density functional theory calculations using a plane wave basis set. *Journal of Chemical Physics* **2010**, *133*.

(99) Spencer, J.; Gajdos, F.; Blumberger, J. FOB-SH: Fragment orbital-based surface hopping for charge carrier transport in organic and biological molecules and materials. *Journal of Chemical Physics* **2016**, *145*.

(100) Lany, S.; Zunger, A. Polaronic hole localization and multiple hole binding of acceptors in oxide wide-gap semiconductors. *Physical Review B* **2009**, *80*, 085202.

(101) Heyd, J.; Scuseria, G. E.; Ernzerhof, M. Hybrid functionals based on a screened Coulomb potential (vol 118, pg 8207, 2003). *Journal of Chemical Physics* **2006**, *124*.

(102) Dudarev, S. L.; Botton, G. A.; Savrasov, S. Y.; Humphreys, C. J.; Sutton, A. P. Electron-energy-loss spectra and the structural stability of nickel oxide: An LSDA+U study. *Physical Review B* **1998**, *57*, 1505-1509.

(103) Anisimov, V. I.; Zaanen, J.; Andersen, O. K. Band theory and Mott insulators - Hubbard-U instead of Stoner-1. *Physical Review B* **1991**, *44*, 943-954.

(104) King, H. F.; Stanton, R. E.; Kim, H.; Wyatt, R. E.; Parr, R. G. Corresponding Orbitals and Nonorthogonality Problem in Molecular Quantum Mechanics. *Journal of Chemical Physics* **1967**, *47*, 1936-1941.

(105) Bylaska, E. J.; Rosso, K. Corresponding Orbitals Derived from Periodic Bloch States for Electron Transfer Calculations of Transition Metal Oxides. *Journal of Chemical Theory and Computation* **2018**, *14*, 4416-4426.

(106) Rettie, A. J. E.; Chemelewski, W. D.; Emin, D.; Mullins, C. B. Unravelling Small-Polaron Transport in Metal Oxide Photoelectrodes. *Journal of Physical Chemistry Letters* **2016**, *7*, 471-479.

(107) Brunschwig, B. S.; Logan, J.; Newton, M. D.; Sutin, N. A semi-classical treatment of electron-exchange reactions - application to the hexaaquoiron(ii)-hexaaquoiron(iii) system. *Journal of the American Chemical Society* **1980**, *102*, 5798-5809.

(108) Kestner, N. R.; Logan, J.; Jortner, J. Thermal electron-transfer reactions in polar-solvents. *Journal of Physical Chemistry* **1974**, *78*, 2148-2166.

(109) Newton, M. D. Formalisms for electron-exchange kinetics in aqueous-solution and the role of *ab initio* techniques in their implementation. *International Journal of Quantum Chemistry* **1980**, *17*, 363-391.

(110) Rosso, K. M.; Dupuis, M. Electron transfer in environmental systems: a frontier for theoretical chemistry. *Theoretical Chemistry Accounts* **2006**, *116*, 124-136.

(111) Guidon, M.; Hutter, J.; VandeVondele, J. Robust Periodic Hartree-Fock Exchange for Large-Scale Simulations Using Gaussian Basis Sets. *Journal of Chemical Theory and Computation* **2009**, *5*, 3010-3021.

(112) Guidon, M.; Hutter, J.; VandeVondele, J. Auxiliary Density Matrix Methods for Hartree-Fock Exchange Calculations. *Journal of Chemical Theory and Computation* **2010**, *6*, 2348-2364.

(113) Paier, J.; Hirschl, R.; Marsman, M.; Kresse, G. The Perdew-Burke-Ernzerhof exchange-correlation functional applied to the G2-1 test set using a plane-wave basis set. *Journal of Chemical Physics* **2005**, *122*.

(114) Lowdin, P. O. Band theory, valence bond, and tight-binding calculations. *Journal of Applied Physics* **1962**, *33*, 251-+.

(115) Hutter, J.; Iannuzzi, M.; Schiffmann, F.; VandeVondele, J. CP2K: atomistic simulations of condensed matter systems. *Wiley Interdisciplinary Reviews-Computational Molecular Science* **2014**, *4*, 15-25.

(116) Dupuis, M.; Watts, J. D.; Villar, H. O.; Hurst, G. J. B. The general atomic and molecular electronic structure system hondo: Version 7.0. *Computer Physics Communications* **1989**, *52*, 415-425.

(117) Hutter, J.; Iannuzzi, M.; Schiffmann, F.; VandeVondele, J. cp2k: atomistic simulations of condensed matter systems. *Wiley Interdisciplinary Reviews: Computational Molecular Science* **2014**, *4*, 15-25.

(118) Humphrey, W.; Dalke, A.; Schulten, K. VMD: Visual molecular dynamics. *Journal of Molecular Graphics* **1996**, *14*, 33-38.

(119) VandeVondele, J.; Hutter, J. Gaussian basis sets for accurate calculations on molecular systems in gas and condensed phases. *J Chem Phys* **2007**, *127*, 114105.

(120) Goedecker, S.; Teter, M.; Hutter, J. Separable dual-space Gaussian pseudopotentials. *Phys Rev B Condens Matter* **1996**, *54*, 1703-1710.

(121) Hartwigsen, C.; Goedecker, S.; Hutter, J. Relativistic separable dual-space Gaussian pseudopotentials from H to Rn. *Physical Review B* **1998**, *58*, 3641-3662.

(122) Zijlstra, E. S.; Huntemann, N.; Kalitsov, A.; Garcia, M. E.; von Barth, U. Optimized Gaussian basis sets for Goedecker–Teter–Hutter pseudopotentials. *Modelling and Simulation in Materials Science and Engineering* **2009**, *17*, 015009.

(123) Rosso, K. M.; Dupuis, M. Reorganization energy associated with small polaron mobility in iron oxide. *J Chem Phys* **2004**, *120*, 7050-7054.

(124) Becke, A. D. Density-functional exchange-energy approximation with correct asymptotic behavior. *Physical Review A* **1988**, *38*, 3098-3100.

(125) Lee, C.; Yang, W.; Parr, R. G. Development of the Colle-Salvetti correlation-energy formula into a functional of the electron density. *Physical Review B* **1988**, *37*, 785-789.

(126) Iordanova, N.; Dupuis, M.; Rosso, K. M. Charge transport in metal oxides: a theoretical study of hematite alpha-Fe2O3. *J Chem Phys* **2005**, *122*, 144305.

(127) Perdew, J. P.; Burke, K.; Ernzerhof, M. Generalized Gradient Approximation Made Simple. *Physical Review Letters* **1996**, *77*, 3865-3868.

(128) Deskins, N. A.; Dupuis, M. Electron transport via polaron hopping in bulkTiO2: A density functional theory characterization. *Physical Review B* **2007**, *75*.

(129) Perdew, J. P.; Burke, K.; Ernzerhof, M. Generalized Gradient Approximation Made Simple [Phys. Rev. Lett. 77, 3865 (1996)]. *Physical Review Letters* **1997**, *78*, 1396-1396.

(130) Lowdin, P. O. Quantum theory of many-particle systems .1. Physical interpretations by means of density matrices, natural spin-orbitals, and convergence problems in the method of configurational interaction. *Physical Review* **1955**, *97*, 1474-1489.

(131) Lippert, G.; Hutter, J.; Parrinello, M. The Gaussian and augmented-plane-wave density functional method for ab initio molecular dynamics simulations. *Theoretical Chemistry Accounts* **1999**, *103*, 124-140.

(132) Lippert, G.; Hutter, J.; Parrinello, M. A hybrid Gaussian and plane wave density functional scheme. *Molecular Physics* **1997**, *92*, 477-487.

(133) VandeVondele, J.; Krack, M.; Mohamed, F.; Parrinello, M.; Chassaing, T.; Hutter, J. Quickstep: Fast and accurate density functional calculations using a mixed Gaussian and plane waves approach. *Computer Physics Communications* **2005**, *167*, 103-128.

(134) Guidon, M.; Hutter, J.; VandeVondele, J. Auxiliary Density Matrix Methods for Hartree-Fock Exchange Calculations. *J Chem Theory Comput* **2010**, *6*, 2348-2364.

(135) Krack, M.; Parrinello, M. All-electron ab-initio molecular dynamics. *Physical Chemistry Chemical Physics* **2000**, *2*, 2105-2112.

(136) Schütt, O.; Messmer, P.; Hutter, J.; VandeVondele, J.: GPU-Accelerated Sparse Matrix-Matrix Multiplication for Linear Scaling Density Functional Theory. In *Electronic Structure Calculations on Graphics Processing Units*, 2016; pp 173-190.

(137) Borštnik, U.; VandeVondele, J.; Weber, V.; Hutter, J. Sparse matrix multiplication: The distributed block-compressed sparse row library. *Parallel Computing* **2014**, *40*, 47-58.

(138) Frigo, M.; Johnson, S. G. The Design and Implementation of FFTW3. *Proceedings of the IEEE* **2005**, *93*, 216-231.

(139) Guidon, M.; Schiffmann, F.; Hutter, J.; VandeVondele, J. Ab initio molecular dynamics using hybrid density functionals. *J Chem Phys* **2008**, *128*, 214104.